

From: FNALD::CAROL 18-FEB-1994 14:08:40.99
To: @CDF_ELECT_DIST.DIS
CC:
Subj: CDF Note No. 1963 Now Available as a PostScript File!

February 18, 1994

Dear CDFers:

You'll find in CDF\$PUB:CDFNOTE_1963.PS a copy of the analysis "Inclusive Photon Cross Section 1992." This is to be blessed at the QCD and Friday meetings in 2 weeks. Enjoy.

Steve Kuhlmann

Inclusive Photon Cross Section 1992

Arthur Maghakian, Steve Kuhlmann, Bob Blair, Rob Harris, Carol Hawk

1 Overview

We present an updated measurement of the inclusive photon cross section using the full 1992-3 data sample. This measurement is a significant improvement over the 1989 measurement due to the addition of the Central Preconverter (CPR) and the neural net hardware trigger improvements.

Contents

1 Overview	1
2 Data Samples	4
3 Background Subtraction Method(s)	4
4 Brief Review of Cuts	5
5 The Results: Direct Photon Cross Section	5
6 Brief Review of Systematic Errors	5
7 Appendix A: The Photon Conversion Probability	6
8 Appendix B: Cross Checks of the Conversion Probabilities	6
9 Appendix C: Backscattered Photons	6
10 Appendix D: Getting Rid of Cosmic Rays: Missing Et Cut	7
11 Appendix E: Trigger Efficiencies	7
12 Appendix F: The No-Track Cut	8
13 Appendix G: The Isolation Cut	8

List of Figures

1	The average number of detected photons in the CPR for each of the different background decay modes.	9
2	The CES and CPR background subtraction “efficiencies” for signal, background, and the data (which presumably is a mixture of both).	10
3	The 1992 inclusive photon cross section compared to the 1989 cross section.	11
4	The 1992 inclusive photon cross section compared with the latest NLO QCD prediction.	12
5	The 1992 inclusive photon cross section compared with the latest NLO QCD prediction. Also shown is a systematic uncertainty band, which is almost 100% correlated.	13
6	The 1992 inclusive photon cross section compared with the latest NLO QCD prediction and variations of renormalization scale.	14
7	The 1992 inclusive photon cross section compared with the latest NLO QCD prediction and variations of parton distributions.	15
8	The Geant pair production cross section divided by the same from the PDG reference Tsai.	16
9	The 2 photon mass distribution, displaying reconstructed π^0 and η mesons and the CPR conversion rates for each.	17
10	A single photon shower in Geant, with a backscattered photon giving a CPR hit.	18
11	The missing Et significance for photons above 70 GeV.	19
12	The missing Et divided by photon Et for photons above 70 GeV.	20
13	The missing Et divided by photon Et for photons from 18-25 GeV.	21
14	The missing Et divided by photon Et for photons from 10-18 GeV.	22
15	The fraction of events failing the missing Et divided by photon Et cut versus photon Et.	23
16	The efficiency of the photon neural net triggers.	24
17	The Et turn-on of the 16 GeV trigger.	25

2 Data Samples

For this measurement we have used the entire 1992 data sample. This sample needs some explanation. There were 3 triggers used, the 50 GeV trigger which did not apply an isolation cut via the neural net L2 hardware, and the 16 and 6 GeV triggers which did. The 50 GeV trigger saw the full 21.85 pb^{-1} luminosity, then Badrun for non-muon analyses brought that down to 20.97 pb^{-1} . The 16 GeV trigger was unrescaled until the final stages of the run when it was prescaled by 2 at high luminosities. This brought the luminosity down to 19.74 pb^{-1} . In addition, there were runs that had to be discarded due to the neural net not working, this reduced the luminosity to 18.14 pb^{-1} . The 6 GeV trigger had a nominal prescale of 300, but ignoring that for the moment it started with 21.70 pb^{-1} , reduced to 20.84 for Badrun, reduced to 18.44 due to additional prescaling at the end of the run, and finally reduced to 16.85 pb^{-1} due to bad neural net runs. This number then needs to be divided by 300 to get the 56.15 nb^{-1} of luminosity in the 6 GeV trigger.

3 Background Subtraction Method(s)

In this note we'll present results using both the standard χ^2 technique and the "new for 92" CPR hit rate (HR) technique. The CPR technique uses the fact that one of the two photons from a π^0 will convert in the coil material around 85% of the time, while a single photon will convert around 60% of the time. The data (a combination of signal and background) will have a HR of around 70%, and the algebra to determine the fraction of single photons from the data is identical to the χ^2 technique. This is given by the following equation:

$$N_\gamma = \frac{(\epsilon_{data} - \epsilon_b)N_{total}}{(\epsilon_\gamma - \epsilon_b)}. \quad (1)$$

Equation 1 comes from $\epsilon_{data}N_{total} = \epsilon_\gamma N_\gamma + \epsilon_b N_B$ with $N_B = N_{total} - N_\gamma$.

The input to this equation, namely the data, background, and signal efficiencies for both techniques are shown in figure 2. The expected CPR conversion rates are derived simply from this equation:

$$\epsilon = 1 - EXP\left(-\frac{7}{9} * X0 * N_\gamma(P_T) * PP\right). \quad (2)$$

where $X0$ is the amount of material in the solenoid coil and PP is the photon pair production cross section which has a slight energy dependence. The term $N_\gamma(P_T)$ is the effective number of photons detected within the CPR "window". The CPR algorithm places a 13 cm window around the photon position as determined by the CES. Clearly for a single direct photon, $N_\gamma(P_T) = 1$, but for low energy π^0 s and η s the separation between the two photons is large enough that only 1 photon is in the "window". We also consider the other multiphoton decays of the η and K_s . These are all displayed in figure 1, which shows the average number of detected photons (in the "window") versus particle P_T . One can see that all the decay modes plateau at high P_T with all the photons being within the window all the time.

4 Brief Review of Cuts

The cuts so far are identical to the 1989 cuts, with two exceptions. We've added a requirement that there is no track pointing at the CPR chamber where the photon candidate is. This is a minor additional cut since we've already required no 3d track in the towers of the candidate, nevertheless the CPR method is quite sensitive to additional particles in the wedge. We have also changed the missing Et cut. Both of these changes and the new cut efficiencies are detailed in the appendices.

5 The Results: Direct Photon Cross Section

The cross section we now present will be a combination of the χ^2 and CPR methods, the χ^2 is used in 1 lonely bin from 10-16 GeV in the 6 GeV trigger, and the CPR everywhere else. The reason for this is that the signal/background is 1/10 at low pt, and the CPR method is statistically weak at low pt. The total statistical plus systematic uncertainty in this bin is smallest right now by using the CES. This was demonstrated in figure 2 by the data efficiencies hugging the background curve at low pt. With more data we'll use the CPR everywhere to reduce our systematic uncertainties. The 1992 cross section is compared with the published 1989 cross section in figure 3. There is good agreement between the two, although it is apparent that the first bin of the 1989 data had fluctuated high.

Figure 4 shows the comparison with NLO QCD prediction. There is a good qualitative agreement over many orders of magnitude. Figure 5 shows the same on a linear scale, along with the systematic uncertainty band that is almost 100% correlated. Figure 6 shows the same on a linear scale, along with changes in renormalization scale. Finally figure 7 displays changes in parton distributions. All the plots show a distinct shape difference between data and theory. The systematic error band is almost 100% correlated, thus the shape change allowed in the data is very small.

6 Brief Review of Systematic Errors

We now assume that in the near future we'll use the CPR in the 6 GeV data, and this method will have much smaller systematics than the CES method. Thus we'll only discuss the CPR systematics here. The main systematic is the uncertainty in the hit rate for photons. The CPR HR has been checked with events with π^0 , η , and ρ peaks, and shows excellent agreement with expectations. This is discussed in detail in appendix B. We take as a systematic 0.01 as the uncertainty on the background conversion rate based on these comparisons, and this translates into a 0.013 uncertainty on the single photon conversion rate. The two are 100% correlated. This is the dominant systematic, being about 6% at 100 GeV and growing to 13% at 16 GeV. This should be compared to the 25-70% systematics in the CES method.

7 Appendix A: The Photon Conversion Probability

For the CPR method the main ingredient is the knowledge in the single photon conversion probability. This includes the true pair production cross section for the materials in the CDF solenoid magnet, the amount of material in the magnet, the number of conversions from the underlying event, dead CPR channels, and the angular effect of going through more material at smaller angles.

For the true pair production cross section we have reviewed the literature, Geant, and EGS. We find that Geant does not reproduce the pair production cross section predicted by the review article by Tsai (reference in the particle data book). Plus the EGS manual says the cross sections in Tsai are more accurate, and the Geant manual admits its cross sections are only good to 5% or so. Given this, we have modified QFL to use the exact cross sections given by Tsai, as this is clearly the most accurate values known. The ratio of Geant to Tsai cross sections is shown in figure 8.

We have done a careful accounting of the material in the solenoid magnet and find there is 1.0748 X0 at 90°, including the outer wall of the CTC and the CDT tubes. This is detailed in CDF 2318 in great detail.

We have measured the number of conversions in minimum bias events as our estimate of the underlying event, and find there is a 3.75% chance of a hit in a 5 channel window. From scanning these events it appears these are soft (10-200 MeV) photons. We correct for this extra hit rate.

We correct for the 0.5% of the CPR that is dead.

We also correct photon by photon for the sin-theta increase in the amount of material at smaller angles.

8 Appendix B: Cross Checks of the Conversion Probabilities

We have 2 sets of cross checks for our signal and background conversion probabilities. They are the reconstructed π^0 and η meson peaks, as shown in figure 9 from cdf2318. These show clear peaks above background and the measured conversion probabilities agree well with the expected. Based on this plot we assign a 0.01 systematic uncertainty to the background conversion probability, which also implies a 0.013 uncertainty on the single photon probability. These two are completely correlated, and give rise to the dominant systematic on the direct photon cross section, 13% at 16 GeV and 6% at 100 GeV.

9 Appendix C: Backscattered Photons

It is possible for low energy photons that are part of the EM shower to travel at very large angles, almost backwards, with respect to the incoming photon. These photons can convert or Compton scatter and give a hit in the CPR, and this effect is not included when considering the normal photon conversions in the solenoid material. We have used Geant to

correct for this. Figure 10 shows an example of 1 event like this. The photons are dashed and the electrons are solid.

10 Appendix D: Getting Rid of Cosmic Rays: Missing Et Cut

Cosmic ray muons can radiate a photon in the CEM and fake a photon signal. The characteristic signature for this is that there is no jet on the other side of the event. We removed these in the 1989 run by a missing-Et significance (missing Et divided by the square root of total Et) cut. The cut was to remove all events with $metsig$ above 3. This is very efficient for lower pt photons, but we've discovered at higher pts when jets hit cracks the significance can be larger than 3. This is demonstrated in figure 11, which shows the significance for photons above 70 GeV. Thus we would either have to have this cut vary with photon Et or do something else. We chose to use a variable used by the dijet and excited quark analyses, the missing Et divided by the cluster Et (or photon Et in this case). Figure 12 shows this variable for photons above 70 GeV, and there is a clean separation with a cut at 0.8. The separation gets worse steadily as you go to lower pt photons, since the jet fluctuations increase, this is shown in figure 13 for photons from 18 to 25 GeV. Clearly there is a tail of real photon events being lost above 0.8, and the figure shows our fitted extrapolation for this loss, which we correct the data for. Below 18 GeV or so you can no longer see the separation between signal and background, this is shown in figure 14. But the fraction of cosmic ray events is getting very small, since the spectrum of cosmic rays is much flatter than direct photons, this is seen in figure 15. The fraction of cosmic rays is dropping rapidly into the few % level down to 10-15 GeV, then it takes off because real direct photons start to be lost at an alarming rate due to the jet fluctuations. Thus we only apply the cut above 18 GeV, and estimate from figure 15 that there is a 2.6% contamination of cosmic rays in the bin from 10-18 GeV, and we correct the photon cross section downward for this.

We take as a systematic uncertainty $1/2$ of the corrections just mentioned, which range from 0 at high pt to 1.3% at 10-18 GeV.

11 Appendix E: Trigger Efficiencies

There are 4 sources of trigger efficiencies, Level 1 not making a 6 GeV seed for the photon, Level2 not making a cluster due to had/em failing, Level2 cluster Et being below the Level2 Et threshold, and the Level 2 neural net isolation failing when it shouldn't. For Level 1 and Level 2 failing had/em we use the studies by Sarah Eno (unpublished as far as we know). She used minimum bias events to study Level 1 and Level1-only events to study Level 2. She found for 9 GeV electrons both of these effects were less than 1%. Since we are only using photons above 10 GeV we will ignore these effects.

Next we treat the neural net. There are 2 ways the neural net can fail when it shouldn't, the first is if the isolation value is above the cut when it shouldn't be due to resolution. The second way is more complicated. The net is fed a seed cluster simply based on the smallest eta position. If the jet opposite the photon is at a smaller eta and makes a 6 GeV seed, then

it will fail the event since it will be non-isolated. This is remedied by using a second neural net board and feed the first two seeds. This second board was added for the last 73% of the data. We can simply use the backup non-neural net triggers to measure these efficiencies. Figure 16 shows the efficiency of both the 1-NNet running and the 2-NNet running and the combination using 27% 1-NNet and 73% 2-NNet. We assign a 2% systematic for this based on the statistical range of possibilities of fits to the 1-NNet data, and the impact of this range on the 1-NNet 2-NNet combination.

Finally we treat the E_t turn-on of the 16 GeV trigger. This is measured by using good electron candidates from the 9 GeV electron trigger, and asking how often the 16 GeV NNet trigger fired versus the electron E_t . This is shown in figure 17. This has been corrected for the nnet efficiencies shown in figure 16, so the E_t turn-on and the neural net efficiency is not double counted. This is why some of the points above 20 GeV go above 100%.

12 Appendix F: The No-Track Cut

Direct photons can fail the no-track cut in 2 ways. First, they can convert in the material in front of the CTC. We use the calibration of this material by the W mass group as 7.51% X0 with a 7% uncertainty. This number changes by very small amounts almost weekly, but this is the latest we have got from them. This leads to a 6% correction to the photon cross section with a 0.4% uncertainty.

The second way direct photons can fail the no-track cut is with a track from the underlying event. We have measured this from minimum bias data to be a 7% correction with a 1% uncertainty. (see CDF2214)

13 Appendix G: The Isolation Cut

We have studied the calorimeter isolation cut using minimum bias data, this is discussed in detail in CDF2214. This efficiency is 78%, with a 3% systematic uncertainty.

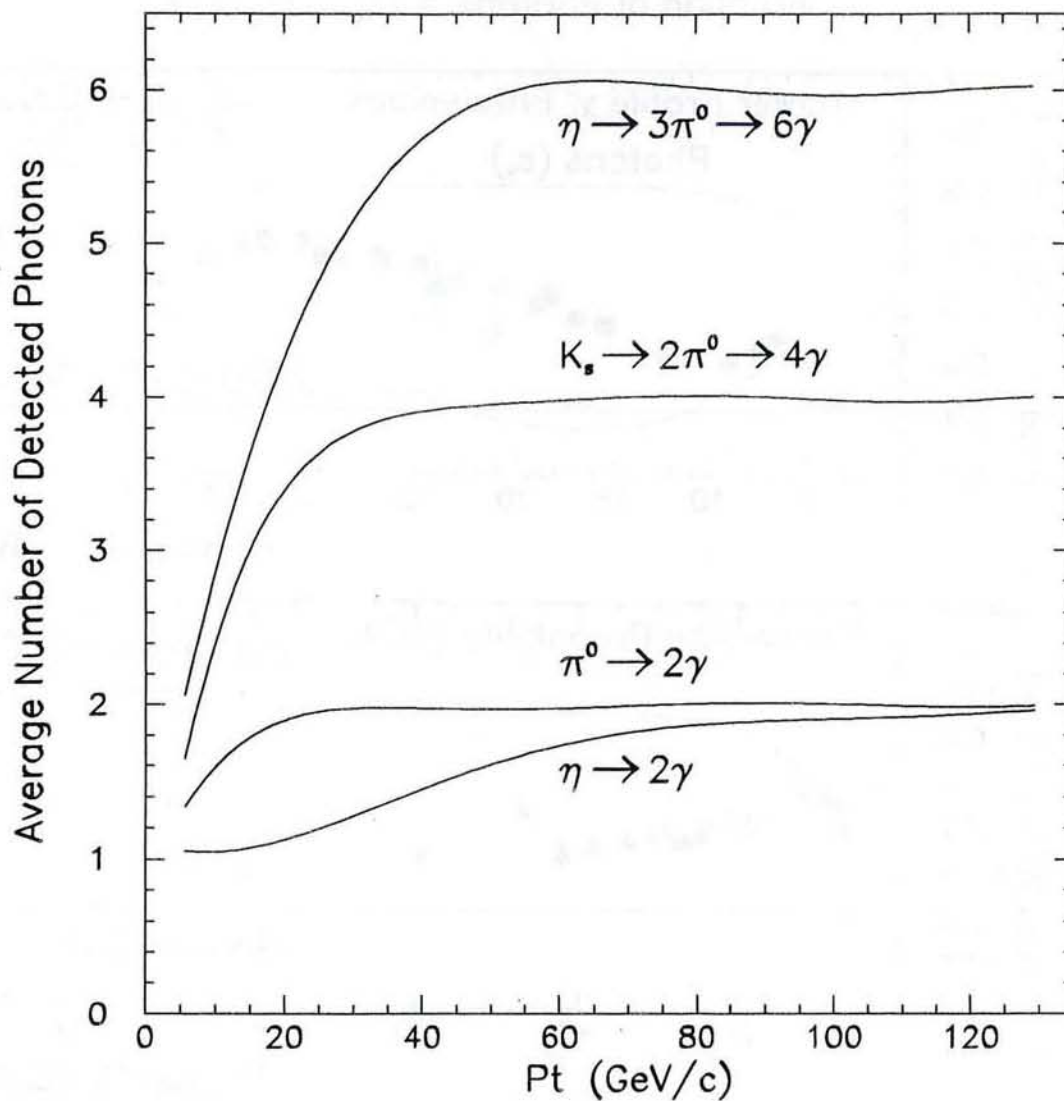


Figure 1: The average number of detected photons in the CPR for each of the different background decay modes.

Background Subtraction Methods

$$\text{Fraction of Photons} = (\epsilon_B - \epsilon) / (\epsilon_B - \epsilon_\gamma)$$

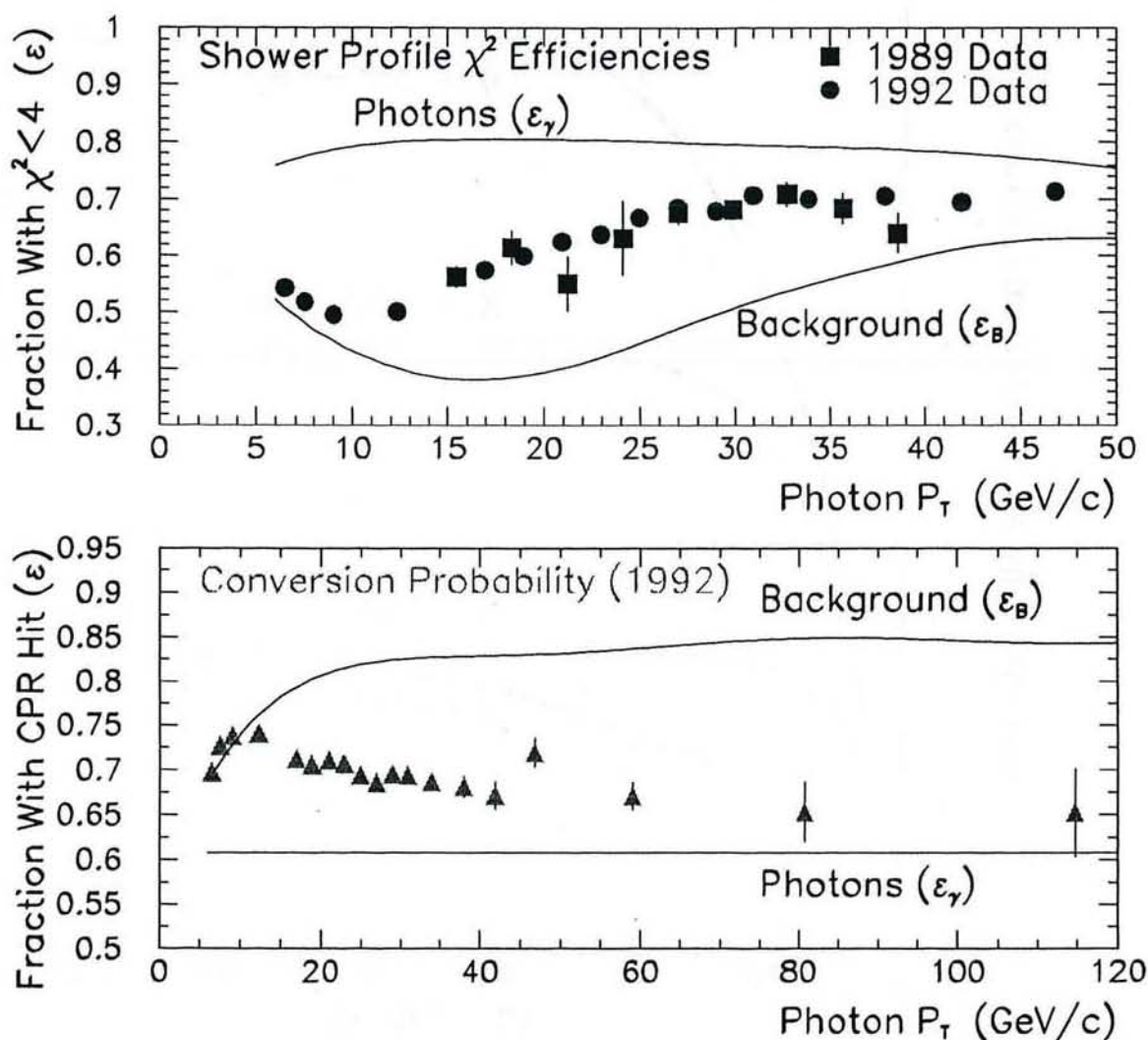


Figure 2: The CES and CPR background subtraction "efficiencies" for signal, background, and the data (which presumably is a mixture of both).

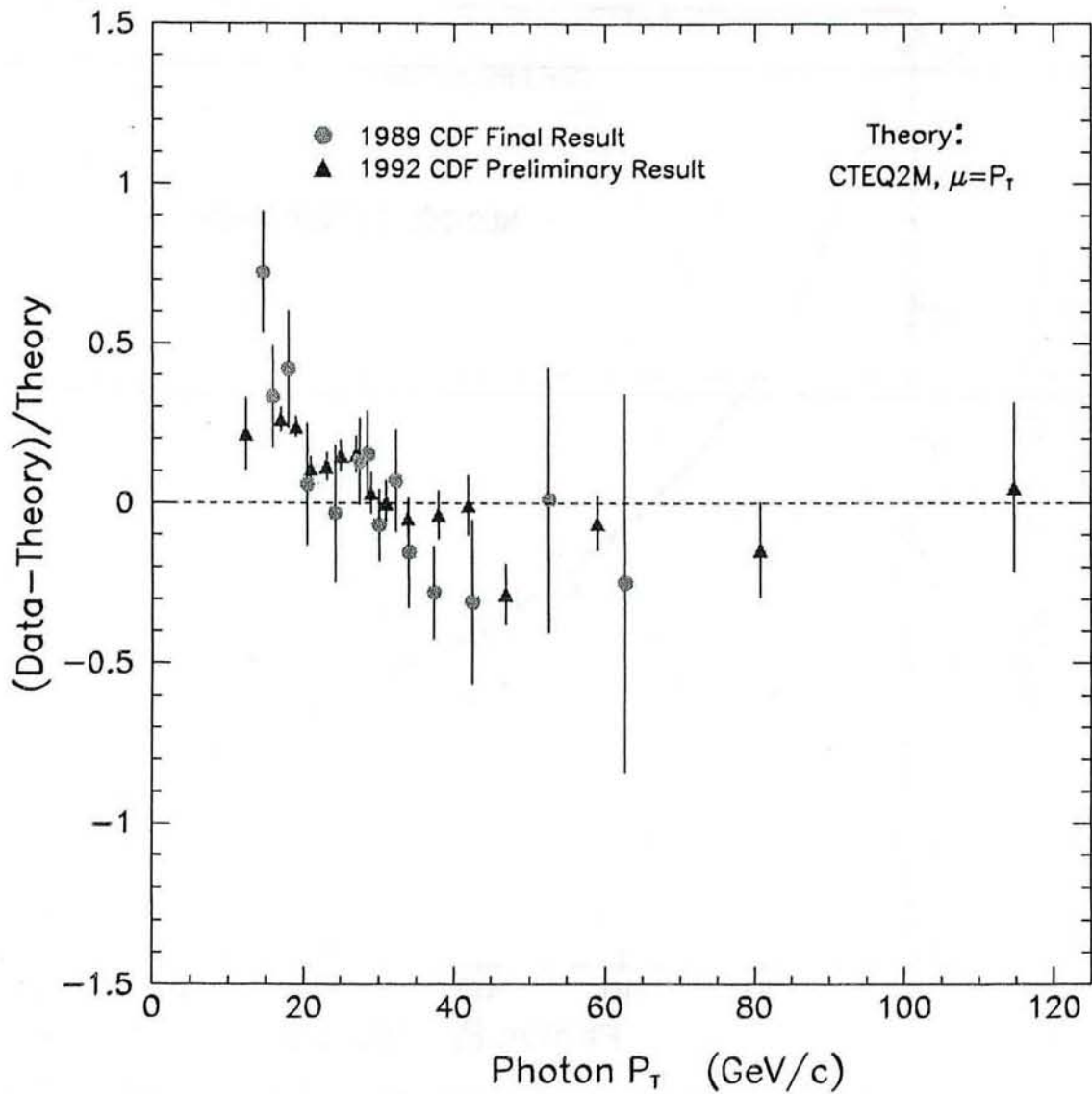


Figure 3: The 1992 inclusive photon cross section compared to the 1989 cross section.

Direct Photon Cross Section

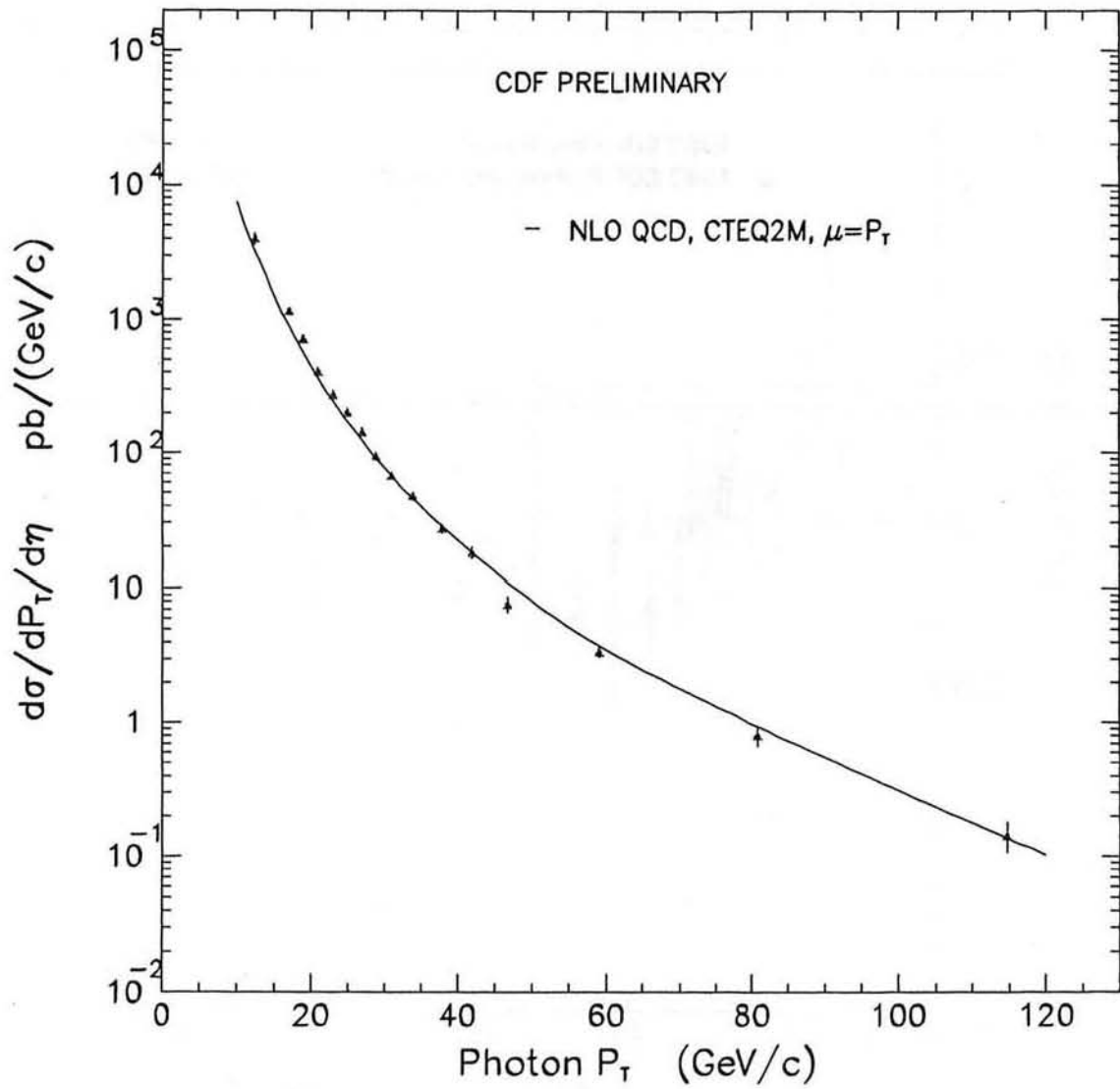


Figure 4: The 1992 inclusive photon cross section compared with the latest NLO QCD prediction.

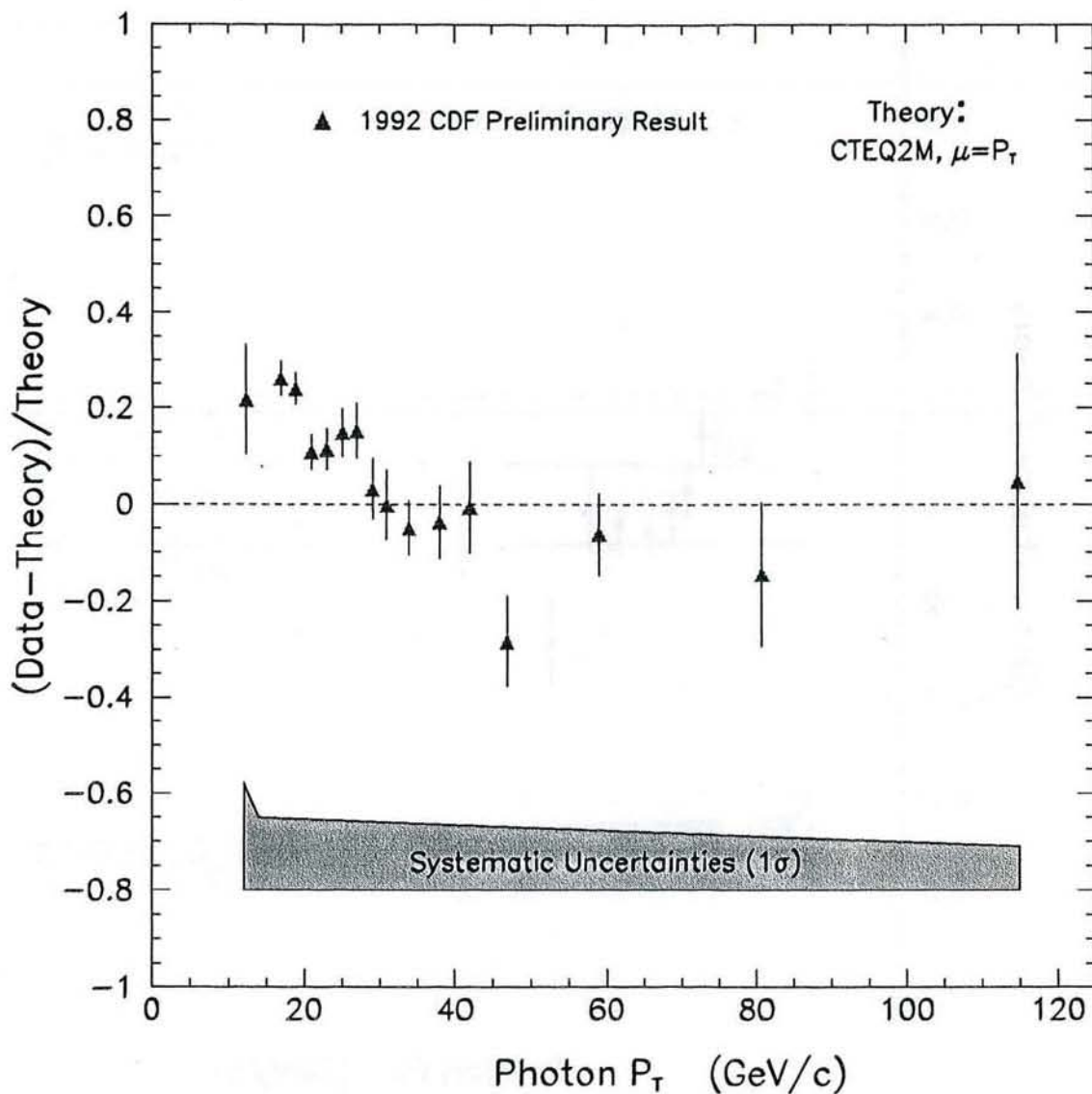


Figure 5: The 1992 inclusive photon cross section compared with the latest NLO QCD prediction. Also shown is a systematic uncertainty band, which is almost 100% correlated.

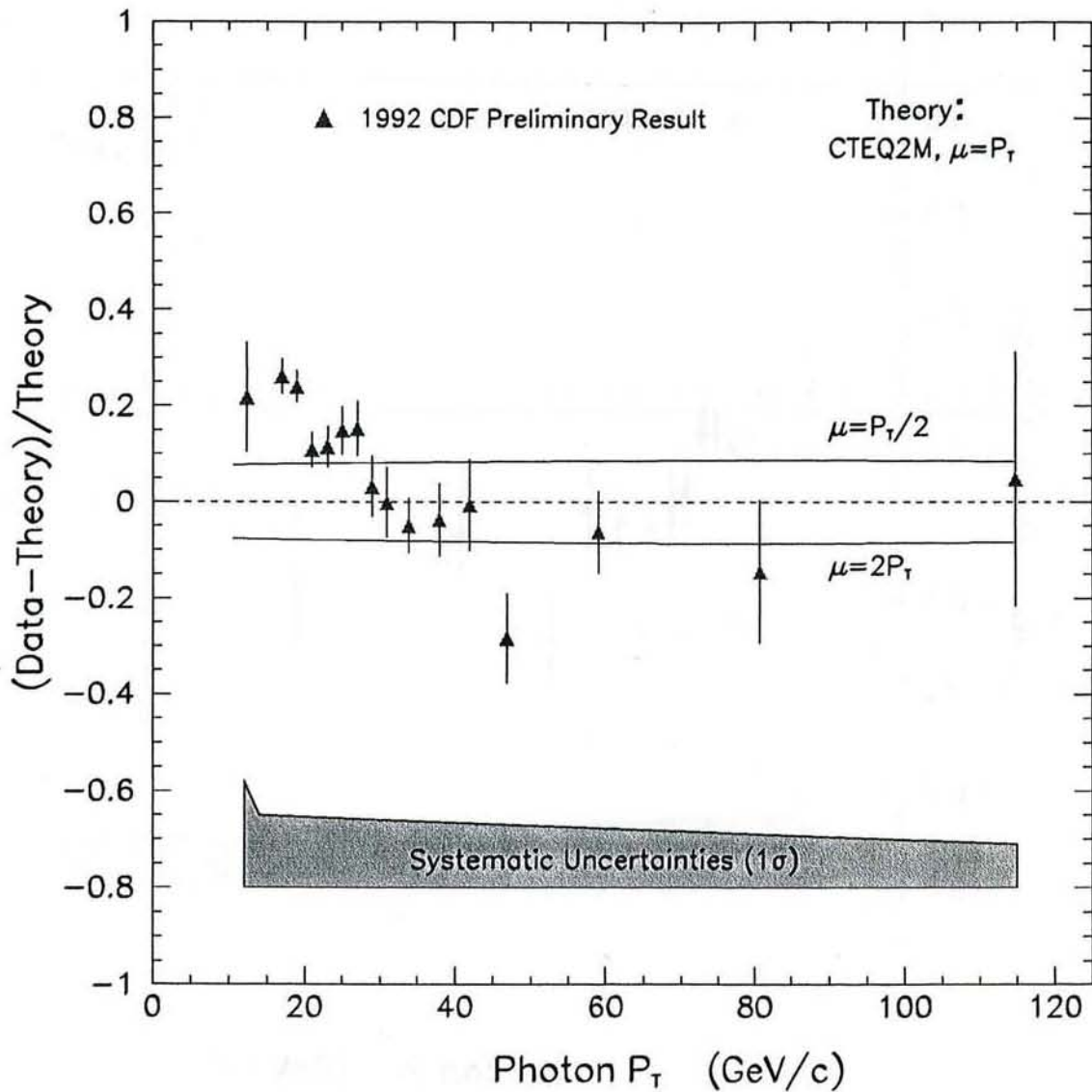


Figure 6: The 1992 inclusive photon cross section compared with the latest NLO QCD prediction and variations of renormalization scale.

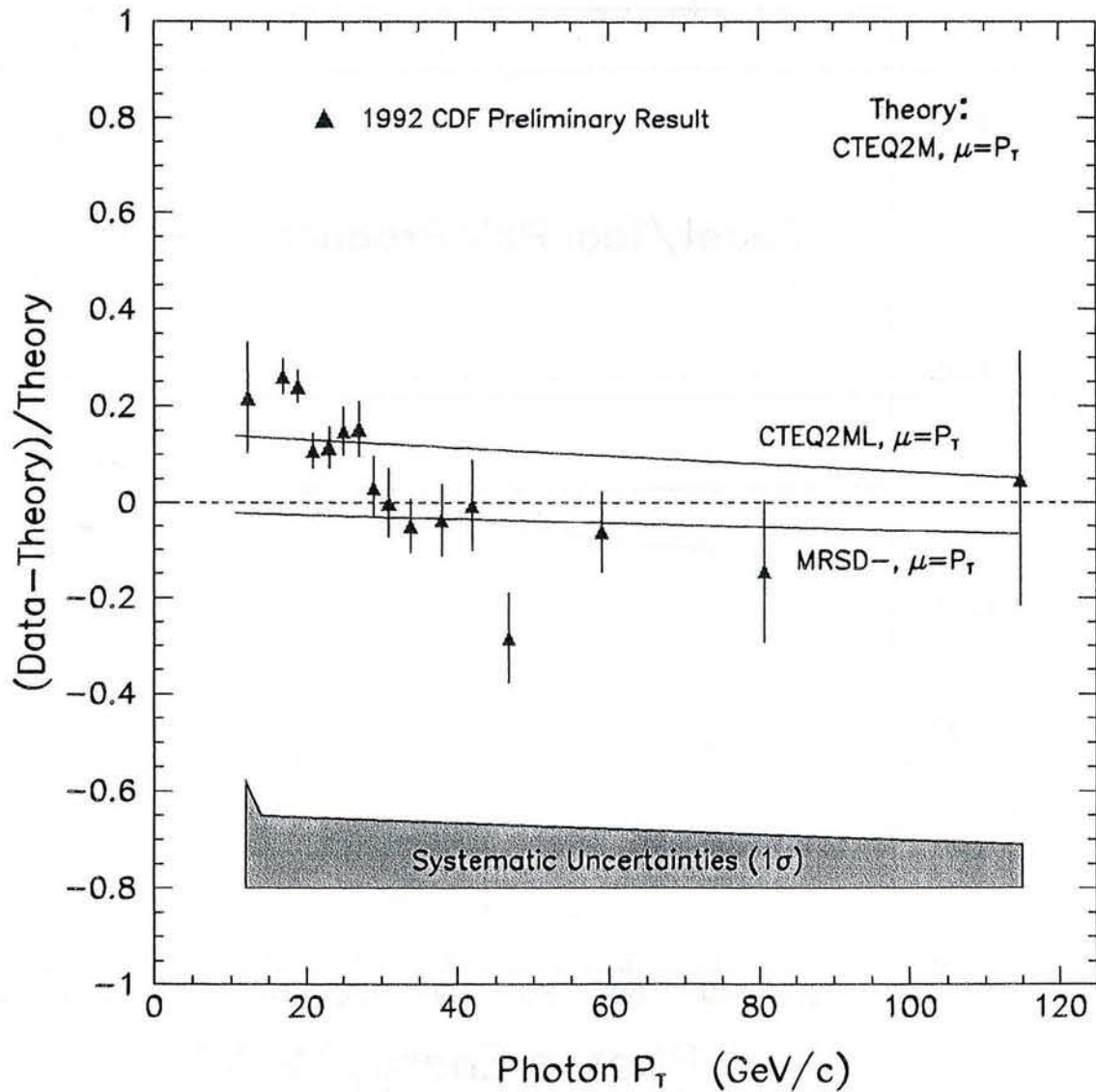


Figure 7: The 1992 inclusive photon cross section compared with the latest NLO QCD prediction and variations of parton distributions.

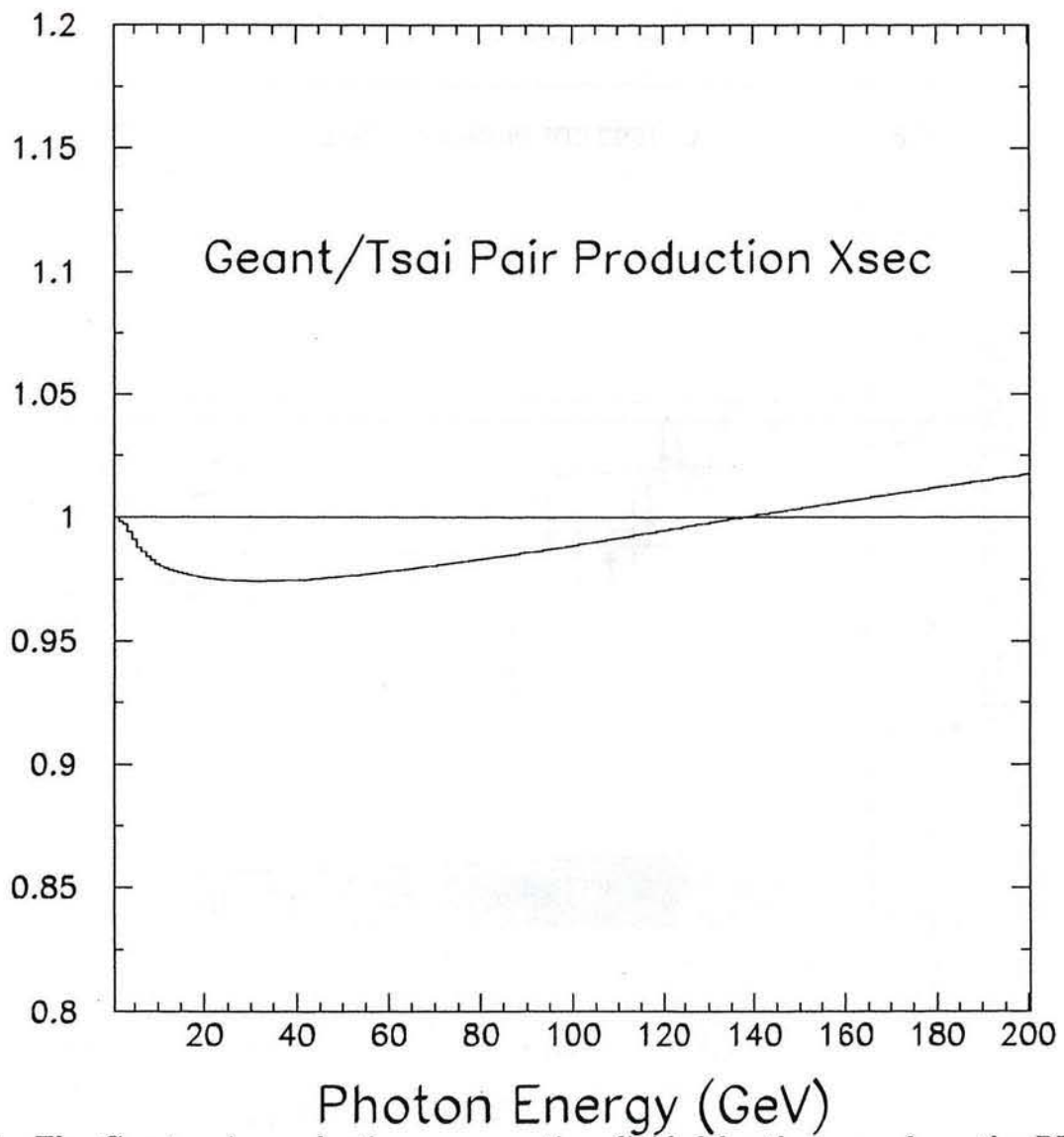


Figure 8: The Geant pair production cross section divided by the same from the PDG reference Tsai.

Calibrating CPR Conversion Probability

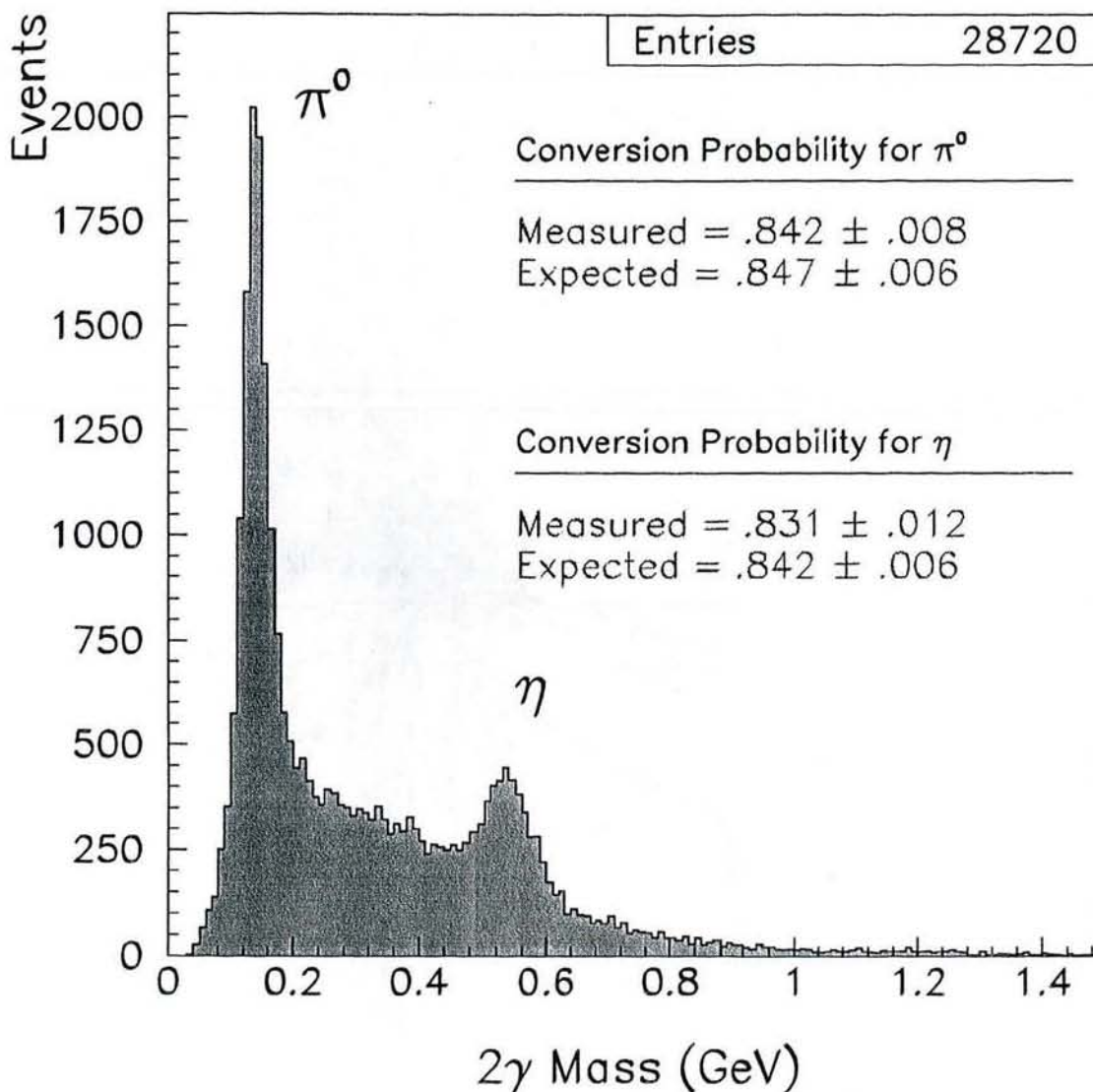


Figure 9: The 2 photon mass distribution, displaying reconstructed π^0 and η mesons and the CPR conversion rates for each.

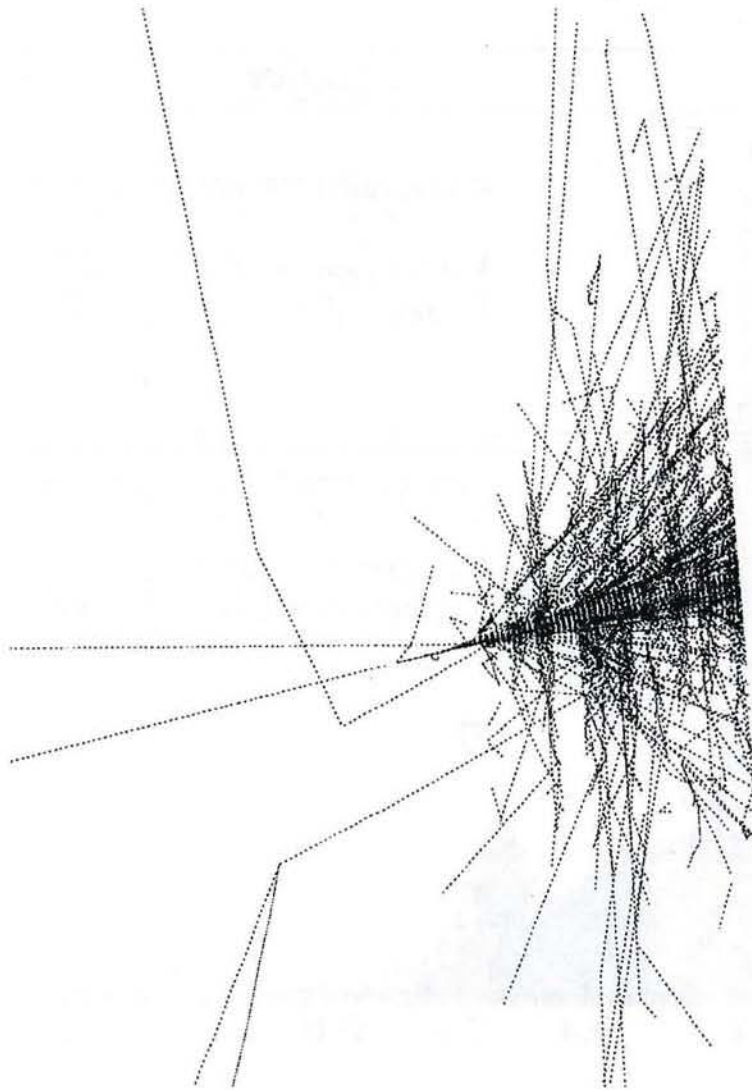


Figure 10: A single photon shower in Geant, with a backscattered photon giving a CPR hit.

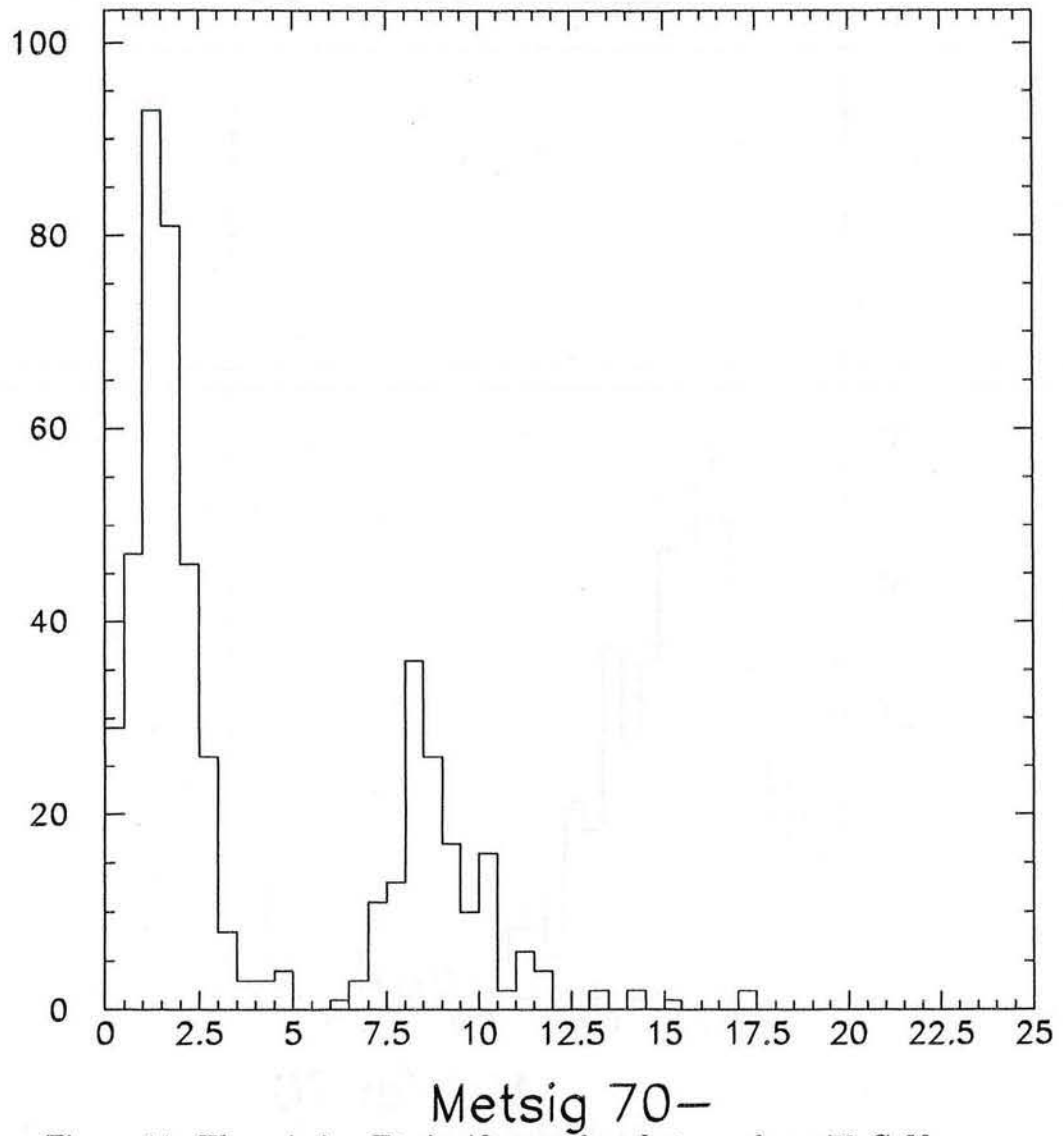


Figure 11: The missing Et significance for photons above 70 GeV.

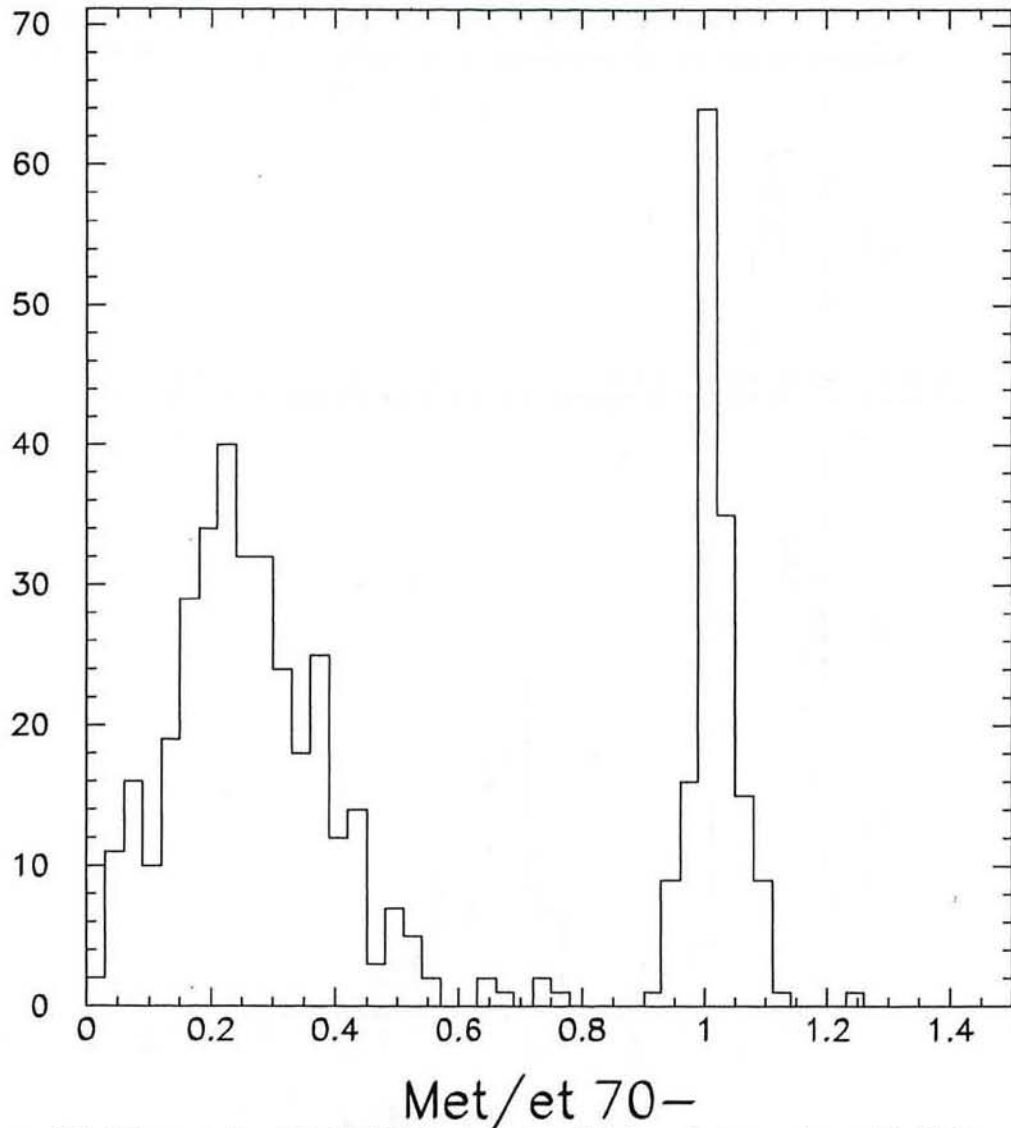


Figure 12: The missing Et divided by photon Et for photons above 70 GeV.

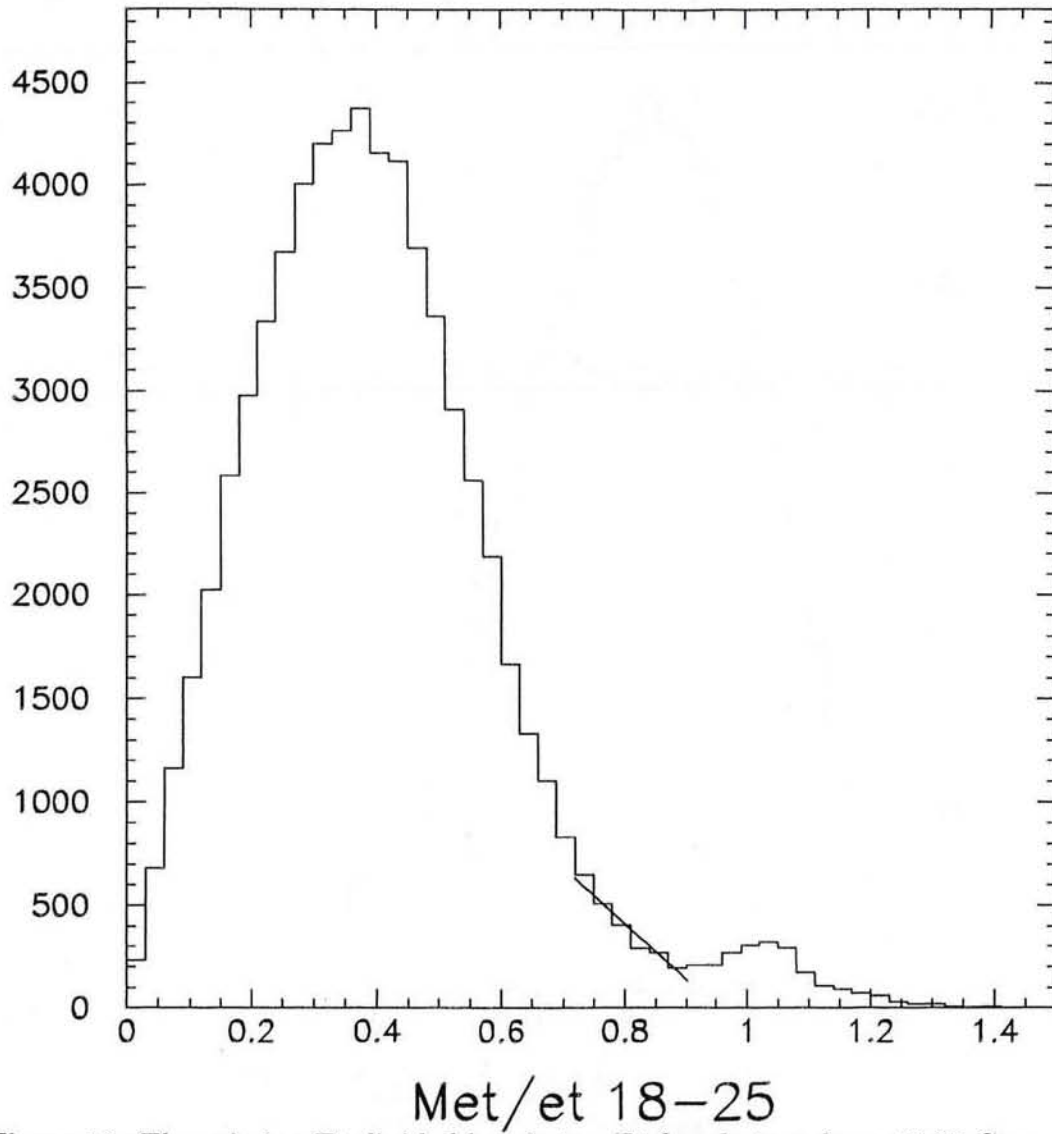


Figure 13: The missing Et divided by photon Et for photons from 18-25 Gev.

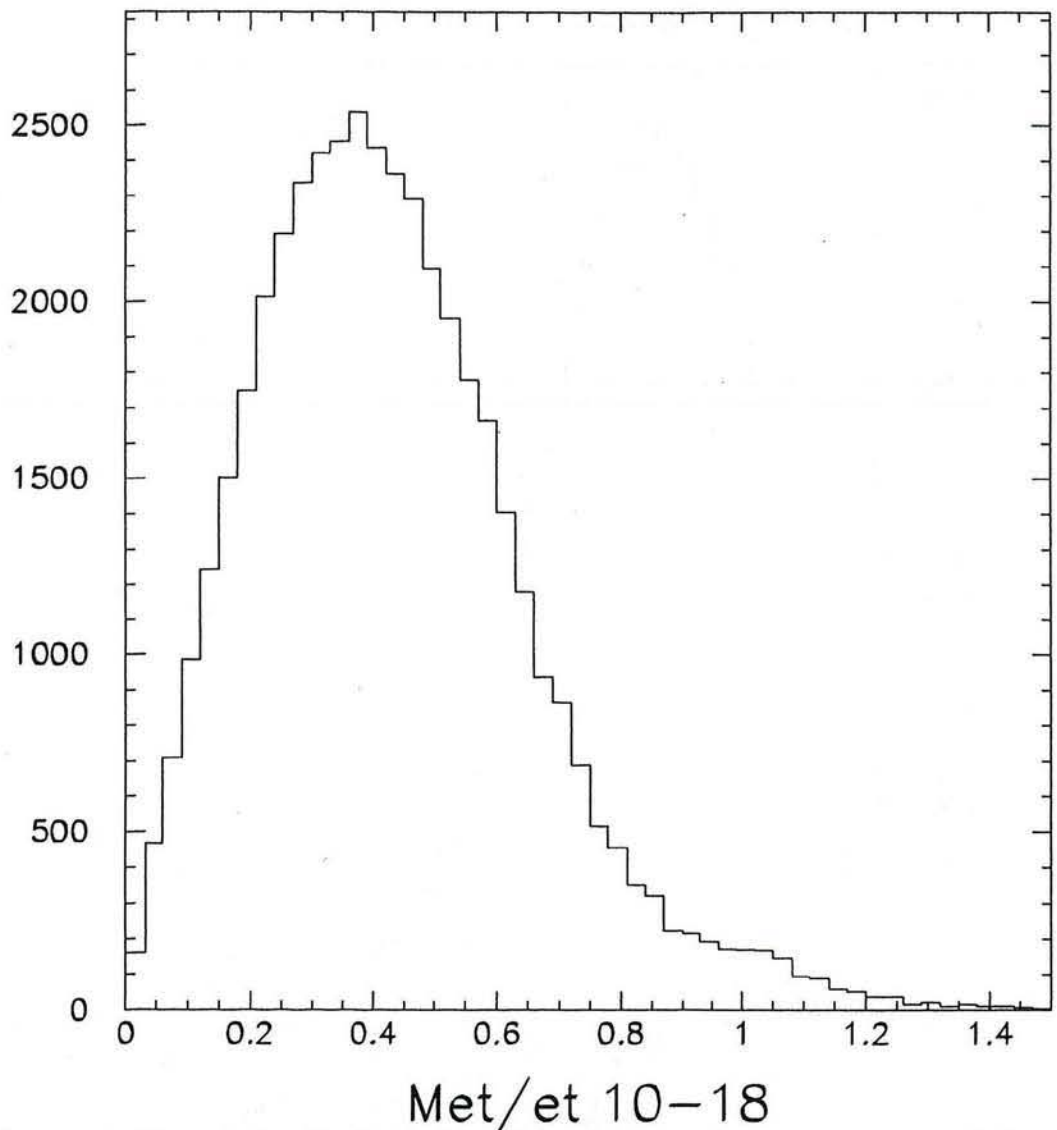
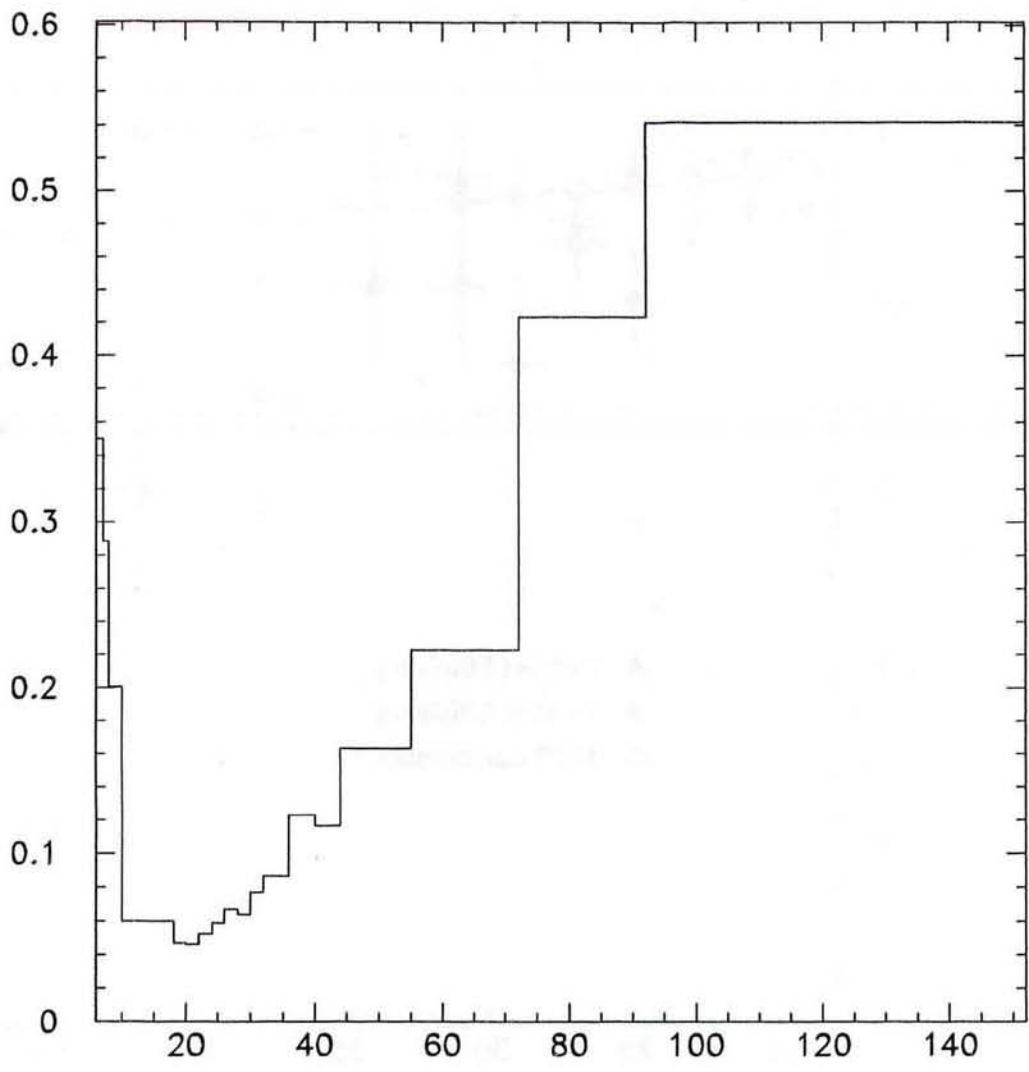


Figure 14: The missing Et divided by photon Et for photons from 10-18 GeV.



Failed Metet cut at 0.8

Figure 15: The fraction of events failing the missing Et divided by photon Et cut versus photon Et.

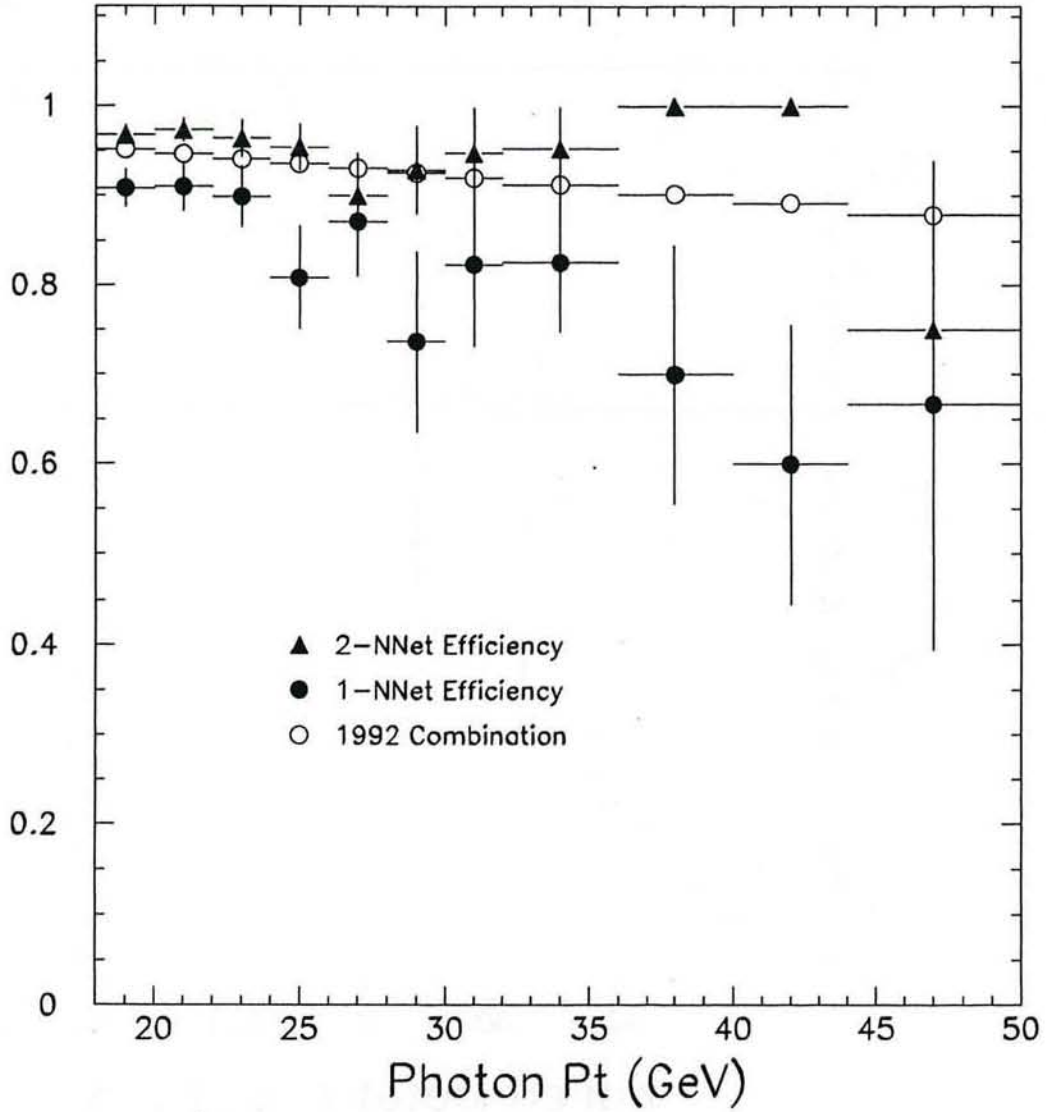


Figure 16: The efficiency of the photon neural net triggers.

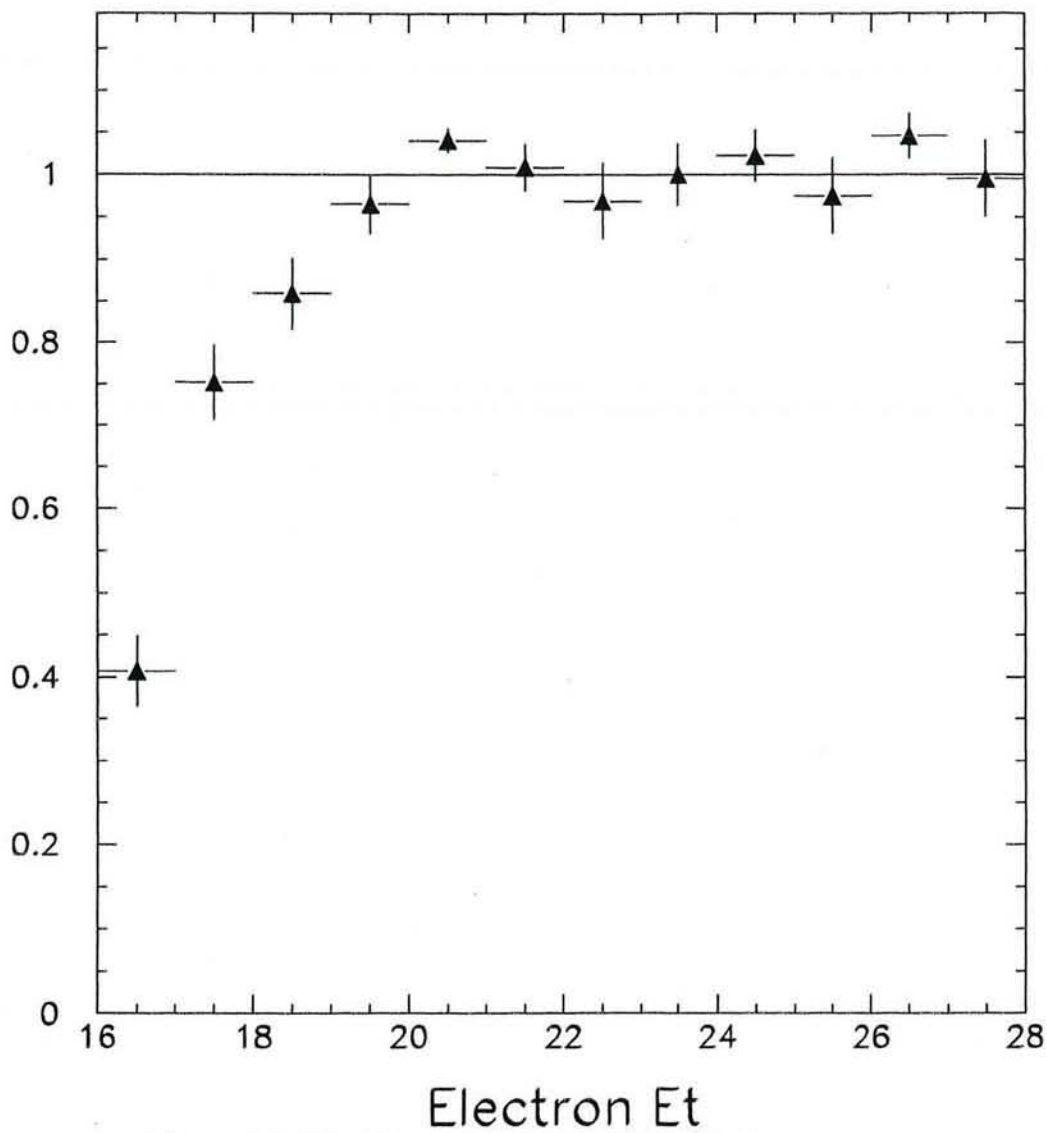


Figure 17: The Et turn-on of the 16 GeV trigger.